La radiologia medica (2026) 131:428–439
https://doi.org/10.1007/s11547-025-02114-8

CARDIAC RADIOLOGY

# Ultrafast non-ECG-gated cardiac spectral CT scanning for myocardial late iodine enhancement assessment: a feasibility study

**Paola Franceschi[1,2] · Camilla Sportoletti[1] · Edoardo Rasciti[1] · Francesco Buia[2] · Domenico Attinà[2] · Fabio Niro[1] · Vincenzo Russo[1] · Luigi Lovato[1]**

Received: 19 August 2024 / Accepted: 22 September 2025 / Published online: 26 November 2025


## Abstract

**Purpose** Evaluate Late Iodine Enhancement (LIE) using the new Philips Spectral CT 7500 scanner without ECG-gating.

**Material and Methods** Fifty-one contrast-enhanced cardiac Computed Tomography (CT) scans with LIE phase (LIE-CT) acquired using the Philips Spectral CT 7500 scanner (8 cm, 256 reconstructed slices) were retrospectively reviewed. LIE-CT was acquired 6–7 min after the administration of contrast agent, using ultra-short scanning time without ECG-gating. LIE-CT technical and dosimetry data were compared with data from 17 cardiac CT scans acquired with Philips Brilliance iCT (4 cm, 128 reconstructed slices). On Spectral CT images, LIE was assessed using "Iodine no water" spectral maps and Extracellular Volume (ECV) quantification. CT findings were compared with the gold standard (Cardiac Magnetic Resonance, CMR) when available.

**Results** Spectral CT images without ECG-gating exhibited high visual quality with minimal motion artifacts. Technical data significantly differed ($p < .001$) between Spectral CT and iCT: median scan time 0.69 s (interquartile range (IQR) 0.66–0.72) vs 8.02 s (IQR 7.32–8.49), median Table speed 433.2 mm/s vs 23.5 mm/s (IQR 21.8–26.5), median CTDIvol 7.2 mGy vs 29.6 mGy (IQR 27.8–33.3), median DLP 211 mGy*cm (IQR 199–222) vs 477.6 mGy*cm (IQR 430.9–551.7), current 812 mA vs 924 mA (IQR 924–925), voltage 100 kV (min 100–max 140) vs 80 kV. Interobserver reproducibility of ECV quantification on Spectral CT images was good in myocardium without LIE and excellent in LIE areas, with negligible bias between observers. Where available, LIE and ECV findings showed good concordance with CMR LGE and ECV.

**Conclusion** Ultrafast non-ECG-gated cardiac Spectral CT provides high-quality images for evaluating LIE, 76% reduction of radiation dose, 50% increase in signal-to-noise ratio, and 91% reduction of acquisition time. ECV measurements demonstrate high interobserver reproducibility. Preliminary findings show good agreement with CMR; while based on a limited validation cohort with selective ECV use.

**Keywords** Detector-based spectral CT · Dual-layer spectral CT · Late iodine enhancement (LIE) · ECG-gating · Dose reduction

## Abbreviations

| | |
|---|---|
| BMI | Body mass index |
| bpm | Beats per minute |
| CA | Contrast agent |
| CCTA | Coronary CT angiography |
| CCTs | Cardiac CT scans |
| CMR | Cardiac magnetic resonance |
| CNR | Contrast-to-noise ratio |
| CT | Computed tomography |
| CTDIvol | Computed tomography dose index |
| DLP | Dose length product |
| ECG | Electrocardiogram |
| ECV | Extracellular volume |
| ECV-CMR | Extracellular volume measured with cardiac magnetic resonance |
| ED | Effective radiation dose |

Vincenzo Russo and Luigi Lovato share the last authorship.

✉ Paola Franceschi
paola.f.franceschi@gmail.com

[1] Pediatric and Adult CardioThoracic and Vascular, Oncohematologic and Emergency Radiology Unit, IRCCS Azienda Ospedaliero-Universitaria di Bologna, Via G. Massarenti, 9, 40138 Bologna, BO, Italy

[2] Department of Medical and Surgical Sciences (DIMEC), University of Bologna, Bologna, Italy

| | |
|---|---|
| ΔHU Myo | Myocardial attenuation difference between pre- and post-contrast scans (Hounsfield Units) |
| ΔHU Blood | Blood pool attenuation difference between pre- and post-contrast scans (Hounsfield Units) |
| ICC | Intraclass correlation coefficient |
| Iodine Myo | Iodine concentration in the myocardium (mg/mL) |
| Iodine Blood | Iodine concentration in the blood pool (mg/mL) |
| IQR | Interquartile range |
| IVS | Interventricular septum |
| LGE | Late gadolinium enhancement |
| LGE-CMR | Late gadolinium enhancement cardiac magnetic resonance |
| LIE | Late iodine enhancement |
| LIE-CT | Computed tomography delayed-phase for late iodine enhancement assessment |
| LIE myocardium | Myocardium with LIE |
| mean HU Pect | Mean attenuation of pectoralis muscle (Hounsfield Units) |
| mean HU Myo | Mean attenuation of healthy myocardium (Hounsfield Units) |
| MINOCA | Myocardial infarction with non-obstructive coronary arteries |
| MOLLI | Modified look–locker inversion recovery |
| MPR | Multiplanar reconstruction |
| non-LIE myocardium | Myocardium without LIE |
| PSIR | Phase-sensitive inversion recovery |
| ROI | Region of interest |
| SBI | Spectral base image |
| SD | Standard deviation |
| SD Pect | Standard deviation of pectoralis muscle attenuation (Hounsfield Units) |
| SNR | Signal-to-noise ratio |

## Introduction

Cardiac magnetic resonance imaging with late gadolinium enhancement (LGE-CMR) is pivotal for the noninvasive characterization of myocardial structure, enabling the identification of extracellular volume (ECV) expansion and myocardial damage patterns [1]. LGE plays a fundamental role in risk stratification, serving as a predictor of adverse cardiovascular events [2]. Accurate and timely identification of myocardial LGE is essential for diagnosing both ischemic and non-ischemic cardiomyopathies and determining optimal clinical management for patients. Despite its undeniable clinical value, LGE-CMR remains limited in availability, particularly in acute settings. Moreover, its application is restricted in certain patient populations, including those with cardiac devices. Although newer devices are MR-conditional, the presence of an implantable cardioverter defibrillator or permanent pacemaker can significantly degrade the quality of LGE images due to artifacts from the device generator [3]. CMR is also unsuitable for patients with claustrophobia or those who cannot tolerate prolonged scanning times. Furthermore, CMR requires electrocardiogram (ECG)-gating, which can be challenging to sample in some patients. Thus, there is a critical need for an effective imaging alternative to LGE-CMR. Recent technological advancements have allowed computed tomography (CT) to evolve from a tool for non-invasive coronary angiography to a modality capable of comprehensive cardiac assessment, including the detection and characterization of myocardial late enhancement. Iodinated contrast agents (CA) exhibit similar kinetics and dynamics to gadolinium chelates, with delayed washout in damaged areas with ECV expansion compared to healthy myocardium. This differential iodine concentration manifests as areas of late iodine enhancement (LIE) on delayed CT scans, 6–7 min post-contrast administration (LIE-CT) [4, 5]. Dual-energy CT has shown promise in visualization and analysis of the LIE, emerging as a viable alternative in patients with contraindications to CMR [4–6]. To our knowledge, existing studies on LIE-CT have exclusively utilized ECG-gated protocols. This study pioneers the use of an ultrafast, non-ECG-gated LIE-CT scan using the Philips Spectral CT 7500 scanner. It aims to evaluate the feasibility of this novel approach in a preliminary setting, using LGE-CMR as the reference standard when available, in a cohort of consecutive, unselected patients.

## Materials and methods

### Study population

All coronary CT angiographies (CCTAs) performed at IRCCS Azienda Ospedaliero-Universitaria di Bologna between February and November 2023 that included a LIE-CT scan were retrospectively reviewed (Fig. 1). Participants were eligible for inclusion if they met all the following inclusion criteria: (1) CCTA with LIE acquisition performed between 1 February 2023 and 30 November 2023, (2) examination carried out on either the Spectral CT 7500 or the Brilliance iCT SP scanner (Philips, The Netherlands), (3) age ≥ 18 years at the time of CCTA. Patients were excluded if they met any of the following exclusion criteria: (1) incomplete imaging data or insufficient image

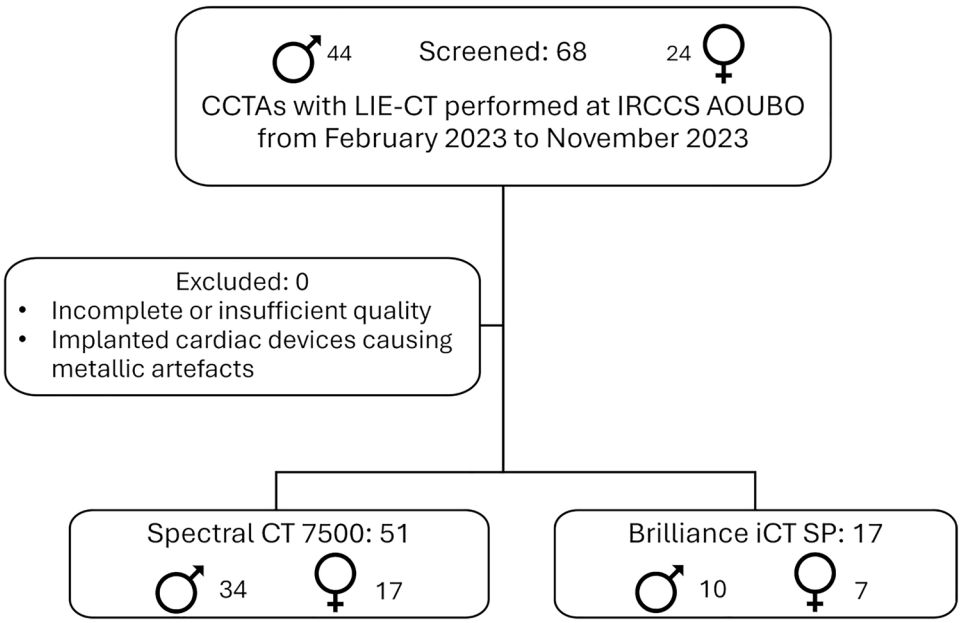


**Fig.1** Study enrollment. Between February 2023 and November 2023, a total of 68 patients underwent coronary computed tomography angiography (CCTA) at IRCCS Azienda Ospedaliero–Universitaria di Bologna. None of the patients were excluded based on the predefined exclusion criteria. Of these, 51 patients underwent CCTA with the Spectral CT 7500 system, while 17 patients were scanned using the Brilliance iCT SP system. CCTA = Coronary Computed Tomography Angiography; LIE-CT = Late Iodine Enhancement Computed Tomography; CT = Computed Tomography

quality for either qualitative or quantitative LIE assessment, (2) presence of implanted cardiac devices causing extensive metallic artifacts that precluded even partial myocardial evaluation, (3) motion-related image artifacts resulting in poor image quality, defined as a score of 4 or 5 on the visual motion-artifact scale described in the Image Analysis section (these artifacts could arise from severe arrhythmias, respiratory motion, or other sources of patient movement during image acquisition). All scans were performed as part of routine diagnostic or follow-up care, and data were collected by reviewing both paper and electronic medical records. Informed consent for imaging was obtained from all patients; the institutional review board waived additional consent for retrospective data analysis.

## Cardiac CT examination

Cardiac CT scans (CCTs) were performed with a dual-layer spectral CT scanner (Spectral CT 7500, Philips, the Netherlands, 8 cm, 256 slices) and a monoenergetic CT scanner (Brilliance iCT SP, Philips, the Netherlands, 4 cm, 128 slices). All patients underwent a standardized scan protocol that included: a non-enhanced ECG-gated scan for the assessment of the calcium score, an ECG-gated contrast-enhanced CCTA using the bolus tracking technique (region of interest in the ascending aorta, threshold 150 Hounsfield Unit (HU)) with retrospective scanning mode, and a LIE-CT acquisition. The LIE-CT scan was performed 6–7 min after CA administration in a craniocaudal direction (from the carina to the diaphragm) during a single breath-hold. Depending on the scanner used, the LIE-CT was acquired either with or without ECG synchronization. Specifically, a non-ECG-gated, high-pitch ultrafast scan was performed using the Spectral CT 7500 system, while an ECG-gated, low-pitch, low-voltage scan was acquired with the Brilliance iCT SP. For the latter, prospective ECG-triggered acquisition was used in patients with a heart rate below 60 bpm (beats per minute), whereas retrospective ECG-gated reconstruction was applied for heart rates above 60 bpm. LIE-CT imaging parameters are fully described in Table 1.

In brief, the newly implemented non-ECG-gated LIE-CT scan with Spectral CT 7500 (Fig. 2) was characterized by a high pitch (1.47) achieved through a high table velocity (433.2 mm/s), a low gantry rotation time (0.27 s) and the thinnest collimation (128 × 0.625 mm). LIE-CT with Brilliance iCT SP requires ECG-gating due to its relatively low pitch (0.18). It is acquired with a low tube voltage (80 kV)

**Table 1** LIE-CT (Late Iodine Enhancement Computed Tomography) images acquisition parameters with Spectral CT 7500 and Brilliance iCT SP. LIE-CT = Late Iodine Enhancement Computed Tomography; CT = Computed Tomography; ECG = Electrocardiogram

| LIE-CT | Spectral CT 7500 | Brilliance iCT SP |
|---|---|---|
| ECG-gating | Non-ECG-gated | ECG-gated |
| Pitch | 1.47 | 0.18 |
| Table velocity range (mm/s) | 405.9–433.2 | 21.8–78.8 |
| Gantry rotation time (s) | 0.27 | 0.27 |
| Collimation (mm) | 128 × 0.625 | 64 × 0.625 |
| Slice thickness (mm) | 2 | 0.67 |
| Gap (mm) | 1 | 0.34 |
| Tube voltage (kV) | 100–140 | 80 |
| Dose modulation | No | Yes |

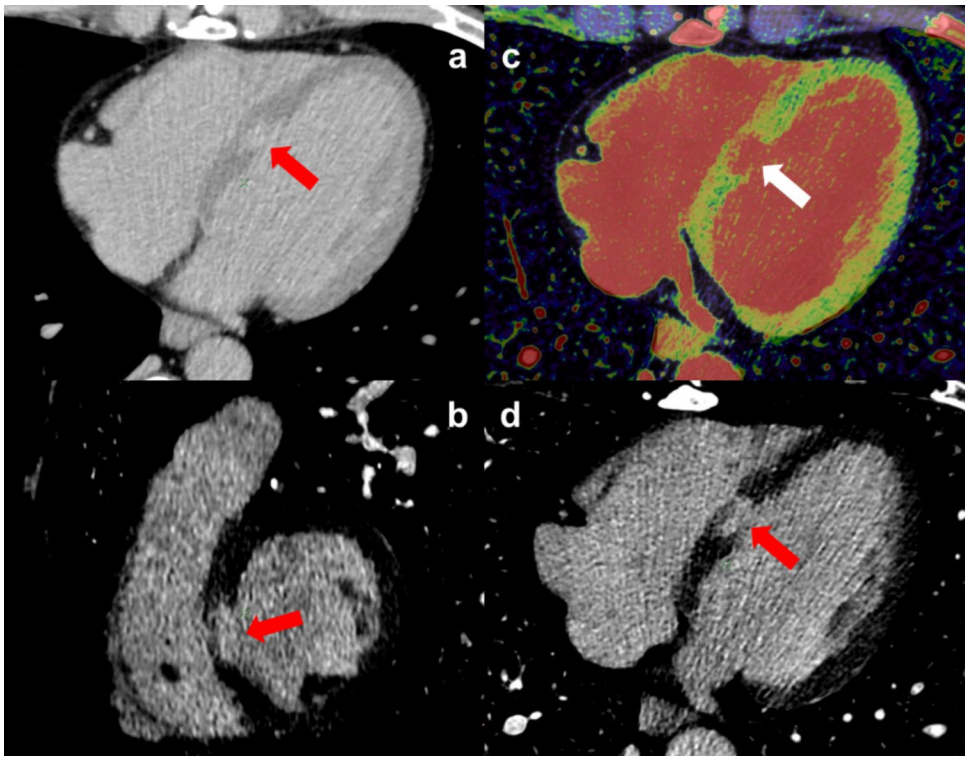


**Fig. 2** Spectral CT 7500 images highlight a mid-interventricular septum area of subendocardial-intramyocardial LIE due to ischemic myocardial damage (red and white arrows). On the ECV spectral map (panel c), two ROIs placed one on the LIE area and one on healthy myocardium showed ECV values of 62% ± 8% and 29% ± 6%, respectively. Panel a, conventional LIE-CT image on axial plane acquired with Spectral CT 7500. Panel b, Iodine-no-water spectral map on two chambers plane. Panel c, ECV spectral map on axial plane. Panel d, Iodine-no-water spectral map on axial plane. CT = Computed Tomography; LIE = Late Iodine Enhancement; ECV = extracellular volume; ROI = Region of Interest; LIE-CT = Late Iodine Enhancement Computed Tomography

and automatic dose modulation (DoseRight, Philips, The Netherlands). Before CCTA, the amount of CA (400 mgI/ml, Iomeron 400, Bracco, Milan, Italy) to be administered was calculated using Certegra P3T Cardiac Software (Bayer, USA). CA was injected through a 16–18 G cannula previously positioned in an antecubital vein at a rate of 4.5–5.0 ml/s, followed by 40 ml saline chaser using a double syringe power injector (Stellant, MedRad, Pittsburgh, USA). Immediately after CCTA, the remaining dose of CA necessary to reach the maximum dose of 100 ml required for LIE evaluation was administered [7]. Before CCTA, all patients received sublingual nitroglycerin before scanning and were given breath-holding instructions before scanning. Patients received oral β-blockers when the heart rate was > 60 beats/min. The acquired volume was then reconstructed using Iterative Model Reconstruction algorithm (IMR1, Philips The Netherlands) and sent to dedicated workstations (IntelliSpace Portal, Philips, The Netherlands).

## Cardiac magnetic resonance examination

CMR was conducted using a scanner Ingenia 1.5 Tesla (Philips, The Netherlands). LGE-CMR was performed 10 min after gadolinium CA injections, with a 2D phase-sensitive inversion recovery (PSIR) gradient-echo pulse sequence employing a modified Look–Locker inversion recovery (MOLLI) sequence to determine the optimal inversion time. LGE-CMR images were acquired in 2-chamber short-axis and long-axis, 4-chamber, and 3-chamber views, as well as planes oriented for specific findings. LGE-CMR 2-chamber short-axis views covered the entire ventricular volumes, with 8 mm slice thickness and no interslice gap. At least one slice was acquired for all other views. Native and 15 min post-contrast T1 mapping data were scanned in identical imaging locations with 3 short-axis slices (apical, mid, and basal portions of the left ventricle). ECV-CMR (Extracellular Volume measured in Cardiac Magnetic Resonance) was semiautomatically measured using dedicated CMR software (cvi42, Circle Cardiovascular Imaging, Calgary, Canada).

## Radiation dose analysis

To assess radiation dose of LIE-CT scans we used volume Computed Tomography Dose Index (CTDIvol) and Dose Length Product (DLP) automatically calculated by the scanner. The effective radiation dose (ED) was calculated using a specific conversion factor for the chest applied to DLP [8], as follows:

$$ED = DLP \cdot 0.014$$

## Image analysis

The technical acquisition data for LIE-CT were collected and compared between scans acquired with Spectral CT 7500 and Brilliance iCT SP. The collected data included:

scan time (s), table velocity (mm/s), CTDIvol (mGy), DLP (mGy*cm), ED (mSv) current (mA), and tension (kV). Additionally, image quality was qualitatively and quantitatively compared between images obtained with the two scanners. In order to evaluate cardiac motion artifacts, myocardium and proximal coronary tracts quality were carefully and independently evaluated by two cardiovascular radiologists and scored in a 1-to-5 point scale as follows: 1, excellent (absence of any motion artifacts); 2, good (minor blurring artifacts); 3, average (moderate blurring or stair-step artifacts); 4, sufficient (significant blurring or stair-step artifacts, limiting diagnostic quality); and 5, poor (non-diagnostic quality). Scans with a score of 4 or 5 would be excluded. For coronary proximal tracts (right coronary artery and left main coronary artery), the one with the worse quality was considered for the score setting. In case of disagreement between observers, examinations were reviewed and consensus was reached. A quantitative analysis of image quality was also performed. Following the methodology described in previously published papers [9–11], HU attenuation of the myocardium was calculated by drawing a Region of Interest (ROI) on LIE-CT axial conventional images at the level of the mid-interventricular septum (IVS) on healthy myocardium. Healthy myocardium was qualitatively defined as a region of myocardium without any apparent LIE. Image noise was defined as the standard deviation (SD) of HU attenuation of an ellipsoid ROI drawn in the pectoralis muscle, placed it at the same level as the IVS ROI, as much as the patient's anatomy allowed. The left pectoralis muscle was chosen for its proximity to the myocardium, with which it likely shares similar noise levels. It was not possible to measure noise at the subscapularis muscle, as previously described [12], because it was not included in the acquired volume. ROI were drawn as large as the thickness of IVS and pectoralis muscle allowed while carefully avoiding, respectively, blood pool and adjacent soft tissues. Signal-to-noise ratio (SNR) was calculated as the mean attenuation of healthy myocardium (mean HU Myo) divided by the image noise [9, 10]:

$$SNR = \frac{mean\,HU\,Myo}{SD\,Pect}$$

The contrast-to-noise ratio (CNR) was calculated by subtracting the mean attenuation of the pectoralis muscle (mean HU Pect) from that of the healthy myocardium (mean HU Myo) and then dividing the result by the image noise (SD Pect) [9, 10]:

$$CNR = \frac{mean\,HU\,Myo - mean\,HU\,Pect}{SD\,Pect}$$

Image noise is inversely related to both image quality and total radiation dose (Fig. 3). Therefore, decreasing SNR and CNR values should correlate with increasing image noise and decreasing image quality. LIE was defined as the presence of hyperattenuating areas within the myocardium compared to adjacent healthy tissue on delayed-phase CT images (acquired 6–7 min after CA administration). In all LIE-CT scans acquired with both the Brilliance iCT SP and the Spectral CT 7500 systems, the presence of LIE was evaluated both qualitatively and quantitatively. Specifically, LIE was visually assessed as either present or absent on conventional images acquired with both scanners by adjusting window level and width settings to optimize the visualization of hyperattenuating regions. For ECV quantification, the CT Multiphase Analysis module of the dedicated software

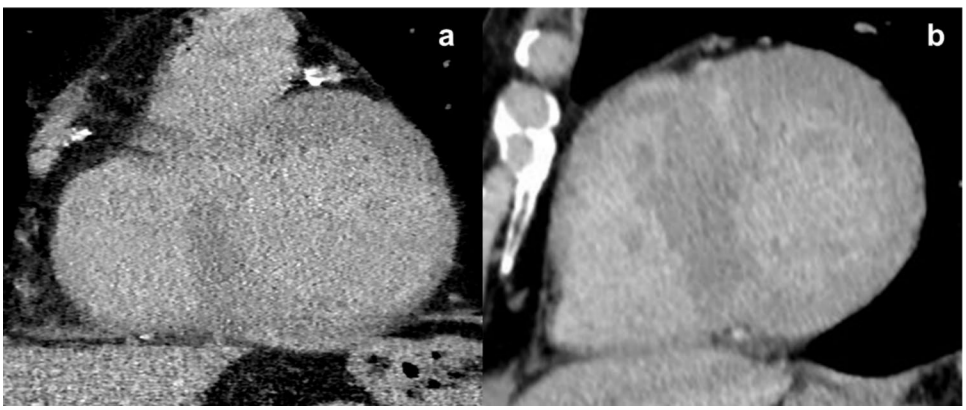


**Fig. 3** Comparison of a conventional LIE-CT image acquired with Brilliance iCT SP (panel a) and a conventional LIE-CT image acquired with Spectral CT 7500 (panel b). Even from a qualitative assessment, the lower noise level in panel b is evident. In panel a, a subendocardial LIE area is faintly visible on the lateral wall, which will become clearer after adjusting window level and width. In panel b, anterior and inferior junctional LIE areas are faintly visible in a patient with hypertrophic cardiomyopathy, better highlighted by Iodine-no-water spectral maps (see Fig. 5). LIE-CT = Late Iodine Enhancement Computed Tomography; CT = Computed Tomography; LIE = Late Iodine Enhancement

IntelliSpace Portal Version 12 (Philips, The Netherlands) was used. This tool enabled ECV calculation using the HU-based method for Brilliance iCT SP (single-energy) CT scans, and the non–HU-based method for spectral CT 7500 scans. For the Brilliance iCT SP system (HU-based method), acquisition of two scans is required: an ECG-gated non-enhanced CT scan and an ECG-gated LIE-CT scan. Attenuation measurements were obtained by placing a region of interest (ROI) within the left ventricular cavity to assess the blood pool, and within the myocardium in the region being examined. The differences in myocardial (ΔHU Myo) and blood pool (ΔHU Blood) attenuation values between the pre- and post-contrast scans were used to evaluate contrast agent distribution, according to the following formula, where Ht denotes the patient's hematocrit:

$$ECV(\%) = (1 - Ht) \cdot \frac{\Delta HU\ Myo}{\Delta HU\ Blood} \cdot 100$$

For spectral CT 7500 scans, ECV is quantified using the non–HU-based method. The spectral separation of late enhancement scans, acquired with energy-sensitive detectors, allows for material decomposition and the generation of iodine maps. This enables quantification of iodine concentration from the Spectral Base Images (SBI) of the LIE-CT scans. With this approach, ECV can be quantified without the need for a non-enhanced acquisition. The equation used for ECV calculation in spectral imaging is as follows, where Ht refers to the patient's hematocrit, and 'Iodine Myo' and 'Iodine Blood' to the iodine concentration in the myocardium and in the blood pool, respectively [13, 14]:

$$ECV(\%) = (1 - Ht) \cdot \frac{IodineMyo}{Iodine\ Blood} \cdot 100$$

For scans performed with the Spectral CT 7500 system, both the "iodine-no-water" maps and the color-coded ECV maps were also visually assessed. For both the HU-based and non–HU-based methods, the Multiphase Analysis software automatically performs image registration across different scan series and normalizes the measured attenuation or iodine concentration values based on a ROI placed in the ascending aorta by the reader. In all patients, ECV values of the myocardium without LIE (non-LIE myocardium) were calculated as the mean of three ROIs placed in the basal, mid, and apical segments of the interventricular septum, taking care to exclude any areas of LIE in LIE-positive patients. In LIE-positive patients, ECV values of the LIE regions were measured by drawing an appropriately sized ROI to encompass the suspected enhancement area. ROIs for ECV quantification were primarily drawn on the axial plane or on the plane that best allowed visualization of the LIE areas. ECV values were interpreted using normal reference ranges according to Yamada et al. [15]. Multiplanar reconstruction (MPR) was employed to generate 2-chamber short-axis views (8 mm slice thickness without gaps) both from LIE-CT conventional and "Iodine no water" images. CMR Phase-Sensitive Inversion Recovery (PSIR) images were assessed for LGE (Figs. 4 and 5). When native and post-contrast T1 sequences were available, ECV-CMR was semi-automatically measured using cvi42 (Circle Cardiovascular Imaging, Calgary, Canada). If areas of LIE on CT and LGE on CMR were identified, their location, distribution, and extent were documented. The concordance between CT and CMR late enhancement findings and ECV measurements was evaluated in myocardial regions with and without LIE or LGE, when both imaging modalities were available. All examinations were reviewed by consensus by two cardiovascular radiologists (4 and 20 years' experience, respectively). Readers were blinded to both the findings from the alternate imaging modality and the clinical data.

## Statistical analysis

Clinical data and data pertaining to image acquisition and quality, LIE-CT, LGE-CMR, and ECV, were summarized for all eligible patients using frequencies and percentages

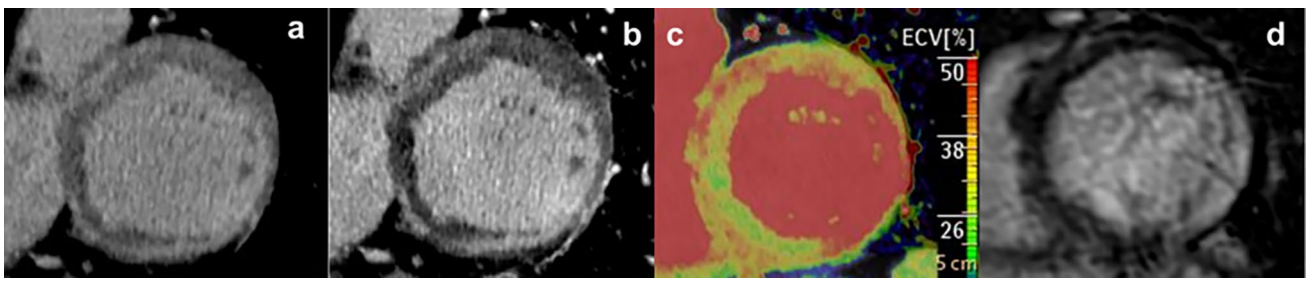


**Fig. 4** Spectral CT 7500 images of a case of dilated cardiomyopathy with ring-like pattern late enhancement, better appreciated on LIE-CT images than on LGE-CMR images. Panel a, conventional LIE-CT image acquired with Spectral CT 7500. Panel b, Iodine-no-water spectral map. Panel c, ECV spectral map. Panel d, LGE-CMR on PSIR image. CT = Computed Tomography; LIE-CT = Late Iodine Enhancement Computed Tomography; LGE-CMR = Late Gadolinium Enhancement Cardiac Magnetic Resonance; ECV = extracellular volume; PSIR = Phase-Sensitive Inversion Recovery

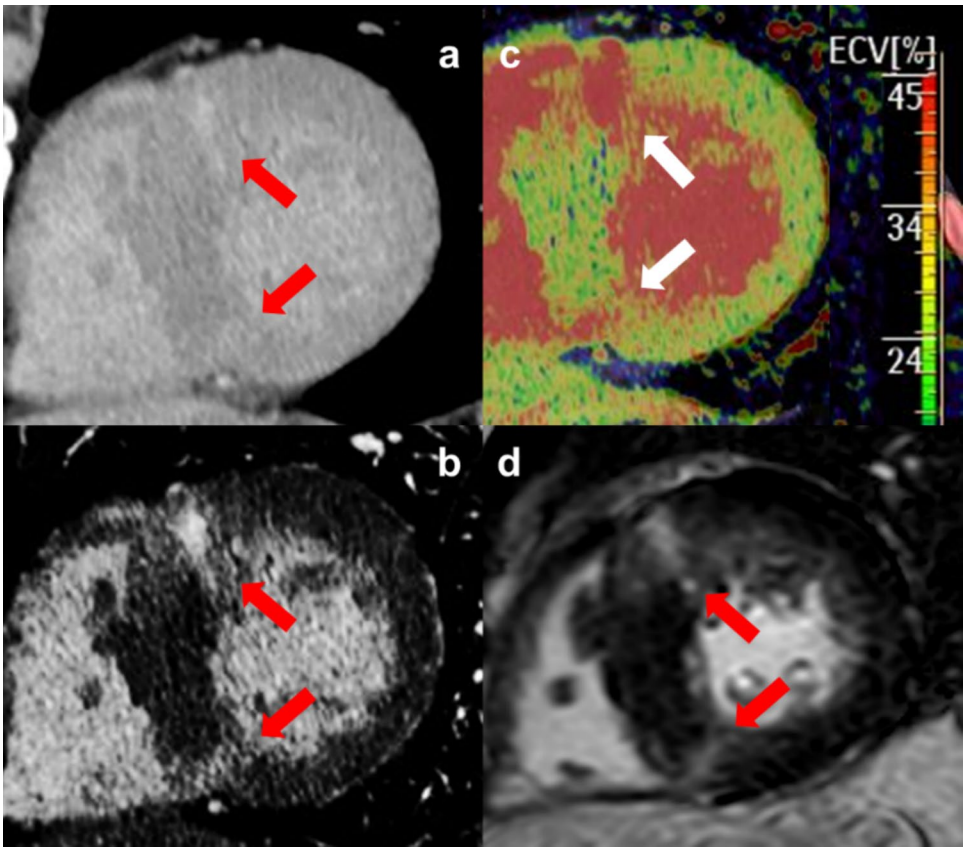


**Fig. 5** LIE-CT images acquired with Spectral CT 7500, and LGE-CMR images of a case of asymmetric hypertrophic cardiomyopathy show anterior and inferior junctional areas of late enhancement (white and red arrows). Late enhancement indicates myocardial damage with fibrotic evolution and has a negative prognostic significance. Panel a, conventional LIE-CT image acquired with Spectral CT 7500. Panel b, Iodine-no-water spectral map. Panel c, ECV spectral map. Panel d, LGE-CMR on PSIR image. LIE-CT = Late Iodine Enhancement Computed Tomography; CT = Computed Tomography; LGE-CMR = Late Gadolinium Enhancement Cardiac Magnetic Resonance; ECV = extracellular volume; PSIR = Phase-Sensitive Inversion Recovery

for categorical variables and median with interquartile range (IQR) for continuous variables. Clinical data and technical data related to the acquisition and quality of late-phase images, expressed as categorical and continuous variables, were compared between patients who underwent Spectral CT 7500 and Brilliance iCT SP using the chi-squared test and the Wilcoxon rank-sum test, respectively, as appropriate. The distribution of image quality scores between the two groups was compared using Fisher's exact test. The Wilcoxon rank-sum test was used to compare ECV values between non-LIE and LIE myocardium in all patients, and between non-LIE myocardium of LIE-positive and LIE-negative patients. The agreement between ECV measurements on ultrafast non-ECG-gated Spectral CT scans performed by two independent readers was evaluated using a two-way intraclass correlation coefficient (ICC) with absolute agreement for single measures, along with Bland–Altman analyses. The ICC values were interpreted as follows: < 0.50, poor; 0.50–0.75, moderate; 0.75–0.90, good; and > 0.90, excellent. A two-sided p value of less than 0.05 was considered to indicate statistical significance. Statistical analyses were performed using Stata V.18 (StataCorp, College Station, Texas, USA).

## Results

### Study patients

A total of 68 patients (24 females, 35%) with a median age of 63 years (IQR 55–72 years) underwent CCT completed by LIE-CT acquisition. Of these, 51 were performed with Spectral CT 7500 and 17 with Brilliance iCT SP. The patients' demographics are shown in Table 2.

All LIE-CT acquisition technical data compared between Spectral CT 7500 and Brilliance iCT SP significantly differ ($p < 0.001$) (Table 3). Specifically, scan time was reduced by 91%, nearly twelve times faster ($p < 0.001$). Radiation dose was reduced by 76% ($p < 0.001$) in terms of CTDIvol, and by 56% in terms of DLP and ED ($p < 0.001$). Qualitative evaluation of image quality indicated that with both scanners, high-quality LIE-CT images without significant motion artifacts (grade 1 out of 5, excellent) were obtained in most cases, 92% and 94% for the Spectral CT 7500 and Brilliance iCT SP, respectively ($p = 0.30$). Only one Spectral CT 7500 scan exhibited moderate motion artifacts (score 3). No scans showed artifacts that limited diagnostic quality or rendered the examination non-diagnostic

**Table 2** Values are expressed as median (interquartile range) or number (%)

| Variable | Total | | Spectral CT 7500 | | Brilliance iCT SP | | *P* value |
|---|---|---|---|---|---|---|---|
| Number of patients | 68 | | 51 | | 17 | | |
| Gender (females (%)) | 24 | (35%) | 17 | (33%) | 7 | (41%) | 0.56 |
| Weight (kg) | 75 | (64–85) | 74 | (64–85) | 78 | (70–82) | 0.56 |
| Height (m) | 1.72 | (1.62–1.80) | 1.71 | (1.62–1.77) | 1.74 | (1.65–1.81) | 0.31 |
| BMI (kg/m$^2$) | 26 | (23–28) | 26 | (23–28) | 25 | (23–27) | 0.70 |
| Heart rate (beats/min) | 60 | (54–67) | 60 | (53–66) | 59 | (54–70) | 0.69 |
| Hematocrit (%) | 41 | (39–43) | 41 | (39–43) | 41 | (39–44) | 0.69 |
| Age at CT scan (years) | 63 | (55–72) | 66 | (58–73) | 60 | (47–69) | 0.11 |
| Time between CT and CMR (days) | 1 | (5–192) | 66 | (46–1555) | 1 | (2–19) | 0.49 |
| Clinical question<br>Ischemic heart disease<br>Myocarditis<br>Non-ischemic—non myocarditis | 47<br>5<br>16 | (70%)<br>(7%)<br>(23%) | 36<br>0<br>15 | (71%)<br>(0%)<br>(29%) | 11<br>5<br>1 | (64%)<br>(29%)<br>(7%) | 0.001 |
| ECV non-LIE myocardium (%) | 26 | (24–28) | 26 | (24–27) | 27 | (26–28) | 0.08 |
| ECV LIE myocardium (%) | 42 | (38–52) | 42 | (40–49) | 44 | (38–55) | 0.90 |
| P value<br>non-LIE vs LIE myocardium | | < 0.001 | | < 0.001 | | < 0.001 | |
| ECV non-LIE myocardium in LIE + patients (%) | 26 | (25–28) | 26 | (24–28) | 28 | (26–28) | 0.13 |
| ECV non-LIE myocardium in LIE—patients (%) | 26 | (24–28) | 26 | (24–27) | 26 | (26–28) | 0.35 |
| P value ECV non-LIE myocardium in LIE + vs LIE—patients | | 0.37 | | 0.95 | | 0.34 | |

Where specified, the range (min–max) is also indicated. CT = Computed Tomography; CMR = Cardiac Magnetic Resonance; BMI = Body Mass Index; ECV = Extracellular Volume; LIE myocardium = myocardium with LIE; non-LIE myocardium = myocardium without LIE

**Table 3** Values are expressed as median (interquartile range) or number (%)

| | Spectral CT 7500 | | Brilliance iCT SP | | *P* value |
|---|---|---|---|---|---|
| Scan time (s) | 0.69 | (0.66–0.72) | 8.02 | (7.32–8.49) | $p < 0.001$ |
| Table velocity (mm/s) | 433.2 | (433.2–433.2)<br>(min 405.9–max 433.2) | 23.5 | (21.8–26.5)<br>(min 21.8–max 78.8) | $p < 0.001$ |
| CTDIvol (mGy) | 7.2 | (7.2–7.2)<br>(min 4.9–max 18) | 29.6 | (27.8–33.3)<br>(min 9.9–max 36) | $p < 0.001$ |
| DLP (mGy*cm) | 211 | (199–222) | 477.6 | (430.9–551.7) | $p < 0.001$ |
| Effective dose (mSv) | 3.0 | (2.8–3.1) | 6.7 | (6.0–7.7) | $P < 0.001$ |
| Current (mA) | 812 | (812–812)<br>(min 236–max 912) | 924 | (924–925)<br>(min 628–max 925) | $p < 0.001$ |
| Tension (kV) | 100 | (min 100-max 140) | 80 | | $p < 0.001$ |
| Image quality:<br>1, excellent (no motion artifacts)<br>2, good (minor artifacts)<br>3, average (moderate artifacts)<br>4, sufficient (artifacts limiting diagnostic quality)<br>5, poor (non-diagnostic) | 47 (92%)<br>3 (6%)<br>1 (2%) | Excellent<br>Good<br>Average | 16 (94%)<br>1 (6%) | Excellent<br>Good | $p = 1.00$ |
| Signal-to-noise ratio | 9.2 | (7.4–11.9) | 4.6 | (3.6–6.8) | $p < 0.001$ |
| Contrast-to-noise ratio | 1.5 | (0.3–2.1) | 1.0 | (0.6–2.2) | $p = 0.48$ |
| IVS ROI area (mm$^2$) | 90 | (70–140)<br>(min 20–max 180) | 60 | (40–80)<br>(min 20–max 150) | $p = 0.005$ |
| Pectoral muscle ROI area (mm$^2$) | 50 | (30–70)<br>(min 7–max 140) | 30 | (20–40)<br>(min 20–max 120) | $p = 0.05$ |

(scores 4 or 5). Quantitative evaluation of image quality demonstrated that in Spectral CT 7500 LIE-CT images SNR was doubled (median SNR = 9.2, p < 0.001) and CNR was generally higher (median CNR = 1.5) although not significantly ($p = 0.48$). The ROIs drawn to define SNR and CNR on the Spectral CT images were larger than those drawn on the Brilliance iCT SP images. Specifically, the IVS ROIs differed significantly ($p = 0.005$), while the pectoral muscle ROIs approached the threshold of significance ($p = 0.05$). All the ROIs were designed to be as large as the thickness of the IVS and pectoral muscle allowed while avoiding adjacent blood pool and soft tissues.

A total of 14 patients were identified with LIE, of whom 8 underwent Spectral CT 7500 and 6 underwent Brilliance iCT SP. Out of 68 patients, 15 also underwent CMR with LGE evaluation. The time interval between CMR and CT scans had an IQR of 5–192 days, with only 4 patients undergoing CMR either more than 5 months before or after CT. Among the 15 patients who underwent CMR (Table 4), 8 had Spectral CT and 7 had Brilliance iCT. The two modalities agreed on the location and distribution of LIE and LGE in all patients except for two, with one false negative in Brilliance iCT SP and one false positive in Spectral CT 7500.

Non-LIE myocardium demonstrated a median ECV of 26% (IQR, 24–28%), significantly lower than that of LIE myocardium (42%; IQR, 38–52%; $p < 0.001$). The difference remained statistically significant when stratified by scanner type (Spectral CT 7500 and Brilliance iCT SP; $p < 0.001$) (Table 2). No significant differences were observed in ECV measurements between the Spectral CT 7500 and the Brilliance iCT SP, in either LIE or non-LIE regions (Table 2). ECV values in the non-LIE myocardium were not significantly different between LIE-positive and LIE-negative patients, both in the overall cohort and when stratified by scanner type (Table 2). Interobserver reproducibility for ECV measured on ultrafast non-ECG-gated Spectral CT scans was good for myocardium without LIE and excellent for areas with LIE, with ICC values of 0.89 (95% confidence interval: 0.81–0.93) and 0.97 (95% confidence interval: 0.79–0.99), respectively. Bland–Altman analyses revealed negligible bias in both groups, with 95% limits of agreement encompassing the null value, indicating no systematic differences between observers. Specifically, for non-LIE myocardium, the mean difference (bias) was − 0.08 with a standard deviation of 1.19 and 95% limits of agreement ranging from − 2.42 to 2.26. For LIE myocardium, the mean difference was − 1.5, with a standard deviation of 1.78 and 95% limits of agreement from − 4.97 to 1.97. ECV values obtained with Spectral CT and CMR were compared in three patients who underwent both imaging modalities and for whom post-contrast T1 mapping sequences (required for ECV-CMR calculation) were available. All three patients showed comparable positive findings for both LIE on CT and LGE on CMR. The difference in ECV values between the two methods did not exceed 3 percentage points in any patient, for either LIE or non-LIE myocardium. Specifically, ECV values for LIE myocardium were 50% vs. 47%, 39% vs. 37%, and 37% vs. 34% on CT and CMR, respectively. For the non-LIE myocardial regions of the same three patients, in the same order, values were 26% vs. 24%, 29% vs. 31%, and 25% vs. 28%. Most of the patients in our study cohort (70%, Table 2) were referred for CT with a clinical suspicion of ischemic heart disease. Of the 14 patients with positive LIE-CT, 71% ($n = 10$) had chronic disease: 36% ($n = 5$) ischemic heart disease, 28% ($n = 4$) non-ischemic/non-myocarditis heart disease, and 7% ($n = 1$) chronic myocarditis. The remaining 29% (n = 4) presented acutely, including 22% ($n = 3$) ischemic heart disease and 7% ($n = 1$) acute myocarditis. In the LGE-CMR-positive cohort ($n = 7$), 43% ($n = 3$) had chronic non-ischemic/non-myocarditis heart disease, while 57% ($n = 4$) presented acutely, the same four patients who were also LIE-CT positive in the acute setting (43% ($n = 3$) ischemic heart disease and 14% ($n = 1$) acute myocarditis). All four acute cases demonstrated concordant LIE on CT, LGE on CMR, and myocardial edema on T2-weighted images.

**Table 4** Patients who underwent CMR. CMR = Cardiac Magnetic Resonance; LIE-CT = Late Iodine Enhancement Computed Tomography; LGE-CMR = Late Gadolinium Enhancement Cardiac Magnetic Resonance

| | Spectral CT 7500 | Brilliance iCT |
|---|---|---|
| Total CMR | 8 | 7 |
| LIE-CT + | 5 | 3 |
| LGE-CMR + | 4 | 4 |

## Discussion

The newly implemented ultrafast non-ECG-gated scan for LIE evaluation acquired with Philips Spectral CT 7500 offers significant advantages. Firstly, the high pitch (1.48) achieved through the high table velocity (up to 433.2 mm/s) and short gantry rotation time (0.27 s) results in an extremely short scan time, averaging less than 0.7 s. This represents a 91% reduction, nearly 12 times faster ($p < 0.001$), compared to the same acquisition using Brilliance iCT SP. This ultrafast scan time is shorter than the duration of a cardiac cycle when the heart rate exceeds 85 bpm, thus benefiting the majority of patients undergoing cardiac CT. Therefore, ultrafast scanning does not require ECG-gating and can be more easily performed in all types of patients with limited risk of motion artifacts. In addition, it offers a significant advantage in

terms of radiation dose, reduced by 76% ($p < 0.001$) in terms of CTDIvol and 56% in terms of DLP and ED ($p < 0.001$). The reduction in radiation dose is particularly significant because LIE-CT Spectral CT 7500 images are acquired at a high pitch and without retrospective ECG-gating. In contrast, LIE-CT image acquisition with Brilliance iCT SP uses a low pitch (0.18), which requires retrospective ECG-gating and low tension (80 kV) but higher tube current, resulting in higher ED. Moreover, the ultrafast non-ECG-gated scan with Philips Spectral CT 7500 produces an improvement in image quality in quantitative terms: SNR is doubled (median SNR = 9.2, $p < 0.001$) and CNR is generally higher (median CNR = 1.5) although not significantly ($p = 0.48$) compared to Brilliance iCT SP images. The qualitative assessment of image quality is comparable between the two scanners, with the majority of scans rated as excellent (no motion artifacts) in both cases (92% for Spectral CT 7500, 94% for Brilliance iCT SP). The use of spectral "Iodine no water" maps, enabled by spectral data acquisition, is crucial for enhancing the visualization of LIE areas and ensuring a high concordance with CMR (the gold standard for late enhancement evaluation). Furthermore, the use of Spectral CT 7500 and dedicated software allows for direct ECV assessment from LIE-CT images, from which virtual non-contrast images are automatically derived. It was noted that the ROIs drawn to define SNR and CNR on the Spectral CT images were larger than those drawn on the Brilliance iCT SP images. Specifically, the IVS ROIs differed significantly ($p = 0.005$), while the pectoral muscle ROIs approached the threshold of significance ($p = 0.05$). Considering that all the ROIs were drawn to match the thickness of the IVS and pectoralis muscle while avoiding adjacent blood pools and soft tissues, and that the patients examined with the two different scanners did not significantly differ in body constitution ($p > 0.05$ for weight, height, and Body Mass Index (BMI)), the observed difference may be attributed to the higher quality of the Spectral CT images. This superior image quality likely increased the radiologist's confidence in avoiding adjacent blood pools and soft tissues, thereby allowing for larger ROIs to be drawn. A statistically significant difference was observed between the ECV values of non-LIE myocardium in the overall cohort and LIE myocardium in LIE-positive patients, with comparable results on the two CT scanners. The ECV values of non-LIE myocardium align with those reported in the literature [15] for healthy subjects. The finding that ECV values in the non-LIE myocardium did not differ significantly between LIE-positive and LIE-negative patients, may suggests that, in our patient cohort, alterations in ECV were unlikely in the absence of visually detectable LIE. Further research with carefully selected patient cohorts is warranted to validate the use of ECV for detecting diffuse myocardial alterations with the ultrafast acquisition technique. The high interobserver reproducibility of ECV measurements (good in non-LIE myocardium (ICC = 0.89) and excellent in LIE myocardium (ICC = 0.97)) along with the absence of significant bias, suggests that ultrafast non-ECG-gated Spectral CT provides consistent and reliable ECV quantification, even in the absence of ECG synchronization. In the 15 patients who had both CT and CMR, all CMRs were acquired within 4 months before or after CT, except for 4 patients, all of whom underwent Spectral CT 7500. Only one of these 4 patients showed discordant LIE-CT and LGE-CMR findings. This patient was categorized as a false positive because the CT scan showed a suspicious LIE area in the inferior apical region not visible on LGE-CMR. Moreover, a review of the patient's clinical history did not reveal other potential causes that could justify the positive result. The other case of CT-CMR discordance was a false negative on Brilliance iCT SP scan, which missed a subendocardial area of LGE-CMR in the mid-basal inferior region, compatible with a scar from a previous myocardial infarction. Both cases of CT-CMR discordance involved areas of late enhancement in the inferior wall, which can be identified as a possible pitfall, particularly in patients who are less compliant with breath-hold instructions. The comparison between ECV measured on CT and ECV-CMR was possible in 3 of the 4 true positive CMR patients who underwent Spectral CT 7500, as the post-contrast T1 mapping sequences required to calculate ECV-CMR were available only in these cases. The difference in ECV values between the two methods did not exceed 3 percentage points in any patient, for either LIE or non-LIE myocardium. Acquiring diagnostic images for LIE-CT and ECV evaluation without ECG-gating allows for the assessment of these parameters in late body scans not acquired specifically for a cardiac indication, with the FOV including the heart but not specifically targeting it. This method eliminates the need for additional scans, thus avoiding extended acquisition times and increased radiation dose. Such an approach can be particularly useful in oncology follow-up patients for evaluating cardiotoxicity and drug-induced myocardial damage [16], and in heart transplant recipients for rejection assessment, as demonstrated for CMR [17]. The study cohort comprised both acute and chronic cases, with the majority being chronic. Acute cases were confirmed by clinical and laboratory evidence and the presence of myocardial edema on CMR in late enhancement areas observed in both CMR and CT. Therefore, like LGE-CMR, LIE-CT represents a pathological expansion of the extracellular volume due to various anatomo-pathological substrates such as fibrosis, edema, or others [1]. The main study limitations are the retrospective design and the limited size of the study cohort. In conclusion, this study demonstrates the feasibility of the newly implemented ultrafast, non-ECG-gated scan using Spectral CT 7500 for LIE evaluation. The technique provides high-quality images with minimal motion artifacts, achieving a

76% reduction in radiation dose, a 50% increase in SNR, and a 91% reduction in acquisition time. It allows assessment of various clinical conditions and different LIE-CT patterns. ECV quantification shows high interobserver reproducibility and remains consistent and reliable even without ECG synchronization. Spectral data acquisition is essential for enhancing LIE-CT visibility (particularly through "iodine no water" maps) and accurate ECV measurement. Preliminary results show good agreement with CMR, despite the limited sample size, underscoring the need for validation in larger cohorts. Overall, this approach offers a promising and efficient alternative for myocardial tissue characterization in routine clinical practice.

**Author contributions** Conceptualization contributed by Paola Franceschi, Vincenzo Russo. Methodology contributed by Paola Franceschi, Vincenzo Russo. Formal analysis contributed by Paola Franceschi. Validation contributed by Paola Franceschi, Camilla Sportoletti, Edoardo Rasciti, Francesco Buia, Domenico Attinà, Fabio Niro, Vincenzo Russo, Luigi Lovato. Data Curation contributed by Paola Franceschi. Writing—original draft contributed by Paola Franceschi. Writing—review and editing contributed by Paola Franceschi, Vincenzo Russo. Visualization contributed by Paola Franceschi, Vincenzo Russo. Project administration contributed by Paola Franceschi, Vincenzo Russo. Supervision contributed by Paola Franceschi, Camilla Sportoletti, Edoardo Rasciti, Francesco Buia, Domenico Attinà, Fabio Niro, Vincenzo Russo, Luigi Lovato.

**Funding** This work received no fundings.

**Data availability** The datasets used and/or analyzed during the current study are available from the corresponding author on reasonable request.

## Declarations

**Competing interests** The authors declare that they have no competing interests.

**Informed consent** All patients provided informed consent before scanning. Requirement for informed consent to use patients' data for research purpose was waived given the retrospective design.



## References

1. Merlo M, Gagno G, Baritussio A et al (2023) Clinical application of CMR in cardiomyopathies: evolving concepts and techniques. Heart Fail Rev 28:77–95. https://doi.org/10.1007/s10741-022-10235-9
2. Kuruvilla S, Adenaw N, Katwal AB et al (2014) Late gadolinium enhancement on cardiac magnetic resonance predicts adverse cardiovascular outcomes in nonischemic cardiomyopathy: a systematic review and meta-analysis. Circ Cardiovasc Imaging 7:250–258. https://doi.org/10.1161/CIRCIMAGING.113.001144
3. Fogante M, Volpato G, Esposto Pirani P et al (2024) Cardiac magnetic resonance and cardiac implantable electronic devices: are they truly still "enemies"? Medicina (Kaunas) 60:522. https://doi.org/10.3390/medicina60040522
4. Oda S, Emoto T, Nakaura T et al (2019) Myocardial late iodine enhancement and extracellular volume quantification with dual-layer spectral detector dual-energy cardiac CT. Radiol: Cardiothorac Imaging 1:e180003. https://doi.org/10.1148/ryct.2019180003
5. Ohta Y, Kitao S, Yunaga H et al (2018) Myocardial delayed enhancement CT for the evaluation of heart failure: comparison to MRI. Radiology 288:682–691. https://doi.org/10.1148/radiol.2018172523
6. Palmisano A, Vignale D, Benedetti G et al (2020) Late iodine enhancement cardiac computed tomography for detection of myocardial scars: impact of experience in the clinical practice. Radiol Med 125:128–136. https://doi.org/10.1007/s11547-019-01108-7
7. Liu P, Lin L, Xu C et al (2022) Quantitative analysis of late iodine enhancement using dual-layer spectral detector computed tomography: comparison with magnetic resonance imaging. Quant Imaging Med Surg 12:310–320. https://doi.org/10.21037/qims-21-344
8. Halliburton SS, Abbara S, Chen MY et al (2011) SCCT guidelines on radiation dose and dose-optimization strategies in cardiovascular CT. J Cardiovasc Comput Tomogr 5:198–224. https://doi.org/10.1016/j.jcct.2011.06.001
9. Pontana F, Duhamel A, Pagniez J et al (2011) Chest computed tomography using iterative reconstruction vs filtered back projection (Part 2): image quality of low-dose CT examinations in 80 patients. Eur Radiol 21:636–643. https://doi.org/10.1007/s00330-010-1991-4
10. Szucs-Farkas Z, Strautz T, Patak MA et al (2009) Is body weight the most appropriate criterion to select patients eligible for low-dose pulmonary CT angiography? Analysis of objective and subjective image quality at 80 kVp in 100 patients. Eur Radiol 19:1914–1922. https://doi.org/10.1007/s00330-009-1385-7
11. Russo V, Garattoni M, Buia F et al (2016) 128-slice CT angiography of the aorta without ECG-gating: efficacy of faster gantry rotation time and iterative reconstruction in terms of image quality and radiation dose. Eur Radiol 26:359–369. https://doi.org/10.1007/s00330-015-3848-3
12. Cornfeld D, Israel G, Detroy E et al (2011) Impact of adaptive statistical iterative reconstruction (ASIR) on radiation dose and image quality in aortic dissection studies: a qualitative and quantitative analysis. AJR Am J Roentgenol 196:W336–W340. https://doi.org/10.2214/AJR.10.4573
13. Dubourg B, Dacher J-N, Durand E et al (2021) Single-source dual energy CT to assess myocardial extracellular volume fraction in aortic stenosis before transcatheter aortic valve implantation (TAVI). Diagn Interv Imaging 102:561–570. https://doi.org/10.1016/j.diii.2021.03.003

14. Nacif MS, Kawel N, Lee JJ et al (2012) Interstitial myocardial fibrosis assessed as extracellular volume fraction with low-radiation-dose cardiac CT. Radiology 264:876–883. https://doi.org/10.1148/radiol.12112458
15. Yamada A, Kitagawa K, Nakamura S et al (2020) Quantification of extracellular volume fraction by cardiac computed tomography for noninvasive assessment of myocardial fibrosis in hemodialysis patients. Sci Rep 10:15367. https://doi.org/10.1038/s41598-020-72417-5
16. Chiocchi M, Cerocchi M, Di Tosto F et al (2023) Quantification of extracellular volume in CT in neoadjuvant chemotherapy in breast cancer: new frontiers in assessing the cardiotoxicity of anthracyclines and trastuzumab. J Pers Med 13:199. https://doi.org/10.3390/jpm13020199
17. Soslow J, Godown J, Bearl DW et al (2022) Cardiac magnetic resonance imaging non-invasively detects rejection in pediatric heart transplant recipients. Circ Cardiovasc Imaging 15:e013456. https://doi.org/10.1161/CIRCIMAGING.121.013456